JOURNAL OF GUIDANCE, CONTROL, AND DYNAMICS
Vol. 19, No. 2, March–April 1996

Improved Tunnel Display for Curved Trajectory Following: Experimental Evaluation

Arthur J. Grunwald*
Technion—Israel Institute of Technology, Haifa 32000, Israel

Improvements of a previously developed tunnel display for curved trajectory following have been experimentally evaluated. A fixed-base simulator study has been carried out, in which eight pilot subjects flew a simplified linearized trim model of a large transport aircraft along eight different curved and descending approach trajectories under various experimental conditions. The purpose of this study was to evaluate an new predictor guidance scheme based on an actively driven predictor reference window. The results showed that, for the larger prediction times, the new guidance scheme yielded a superior performance as compared to the original configuration, in which a nonactive predictor reference window was used. Corner cutting, as experienced in earlier configurations, was eliminated, resulting in a highly improved positional accuracy in transitions from straight to curved trajectory sections and back. Furthermore, cross track errors, resulting from low-frequency disturbances, such as slow-varying crosswinds, were greatly reduced as a result of the integral control action imparted to the predictor reference window, without affecting the task difficulty. Subject response has been found to strongly resemble the one of a well-designed autopilot.

Introduction

THE tunnel display layout, used in the experimental program is an improved version of earlier work.[1–3] The layout of the display is shown in Fig. 1a and the horizontal situation in Fig. 1b. The purpose of this display is to allow the pilot to fly a complex curved and descending trajectory, with minimal control effort and workload, while providing a high level of situational awareness. Figure 1a shows the tunnel structure, composed of the four dashed, curved corner lines. The tunnel has a constant square cross section of dimensions 300 × 300 ft. The pilot's task is to keep the aircraft centered within the tunnel, where the sides of the tunnel depict the allowed lateral and vertical deviations from the curved trajectory.

Flight-path centered integrated command displays, providing both the accuracy of flight-director guidance and a high degree of situational awareness, are not new.[4,5] Bray[6] and Bray and Scott[7] investigated these concepts for terminal operations with conventional aircraft, Merrick[8] for curved, decelerating approaches to shipboard landings, and Hynes et al.[9] for precision approaches of powered-lift aircraft along complex, curved trajectories. This paper extends the concepts of these references, in the sense that it focuses on the precision flying of constantly curved trajectory sections and the transitions to and from these sections, and on maintaining a high level of positional accuracy in the presence of slowly varying disturbances.

The success of the earlier tunnel display version can be attributed to a useful combination of the perspective tunnel image with the overlaid predictor symbol P, as seen in Fig. 1a. This predictor symbol represents a point on the predicted vehicle path, at the distance D_p ahead, or T_p seconds in the future; see Fig. 1b. The tunnel image provides the situational awareness and preview of the trajectory forcing function, and the predictor symbol provides the vital guidance and control information necessary for stabilizing the system. It has been shown in earlier work that for a well-chosen prediction time T_p, a control strategy aimed at keeping the predictor P centered at the tunnel cross section square S results in a fast and adequately damped closed-loop system. In fact, the tunnel cross section is equivalent to a ghost aircraft,[9] functioning like a leader aircraft, flying a perfect approach T_p seconds ahead, whereas the predictor is equivalent to a flight-path acceleration symbol.[9]

It might appear though that the tracking task involved in keeping the predictor on the tunnel cross section square might impair the situational awareness by focusing the pilot's attention at the central area of the display. In contrast to the compulsory information provided by flight directors, however, the information provided to the pilot by the predictor is optional. This, for example, allows the pilot to leave the predictor for several seconds to scan other parts of the display to return to it later. Moreover, past experience with this tunnel-with-predictor display has shown that a well-tuned predictor yields a significant reduction of pilot workload. Contrary to what would be expected, this enables the pilot to allocate his or her resources to the spatial awareness, rather than to attempting to track the tunnel with insufficient guidance information.

The improved guidance scheme, discussed in the theoretical companion paper,[10] is being evaluated experimentally. This scheme is aimed at improving the positional accuracy in transitions from straight to curved trajectory sections and back. Furthermore, it employs an appropriate amount of integral control action to reduce cross track errors resulting from low-frequency disturbances, such as slow-varying crosswinds or measurement biases. Since the guidance scheme determines the transfer function of the effectively controlled element, excessive integral control action could adversely affect the tracking workload. An increased workload, in turn, might impair the spatial awareness, since the pilot might need to allocate more attention to the tracking task than to the overall aircraft spatial situation. Therefore, the guidance scheme should be designed so that the tracking workload on the pilot is not affected.

Display Improvements

The geometry of the predictor is shown in Figs. 1a and 1b. Both the predictor and the tunnel square are moving along with the aircraft at a constant prediction time T_p ahead. In this experiment, the prediction time is varied between 3 and 9 s. A second square is drawn at 2 s ahead, as shown in Fig. 1a. This square accommodates the lateral and vertical deviation indicators that display the actual displacements at a scale enlarged by a factor of 2.5. Thus, when the indicators are at the right edge and top edge of the square, the aircraft is 60 ft to the right and 60 ft above the desired trajectory. The bottom shaded area in Fig. 1a depicts the ground plane and the top nonshaded area the sky. Since the ground plane extends to infinity, the separation between the two areas depict the true horizon.

Similar to the geometry of the original tunnel display,[1] the predictor cross represents a point on the circular predicted vehicle path, see Fig. 1b. Thus, the cross depicts the anticipated future vehicle position and the tunnel cross-section square the desired future

Received Nov. 17, 1993; revision received June 30, 1995; accepted for publication Oct. 5, 1995.

*Associate Professor, Faculty of Aerospace Engineering. Member AIAA.

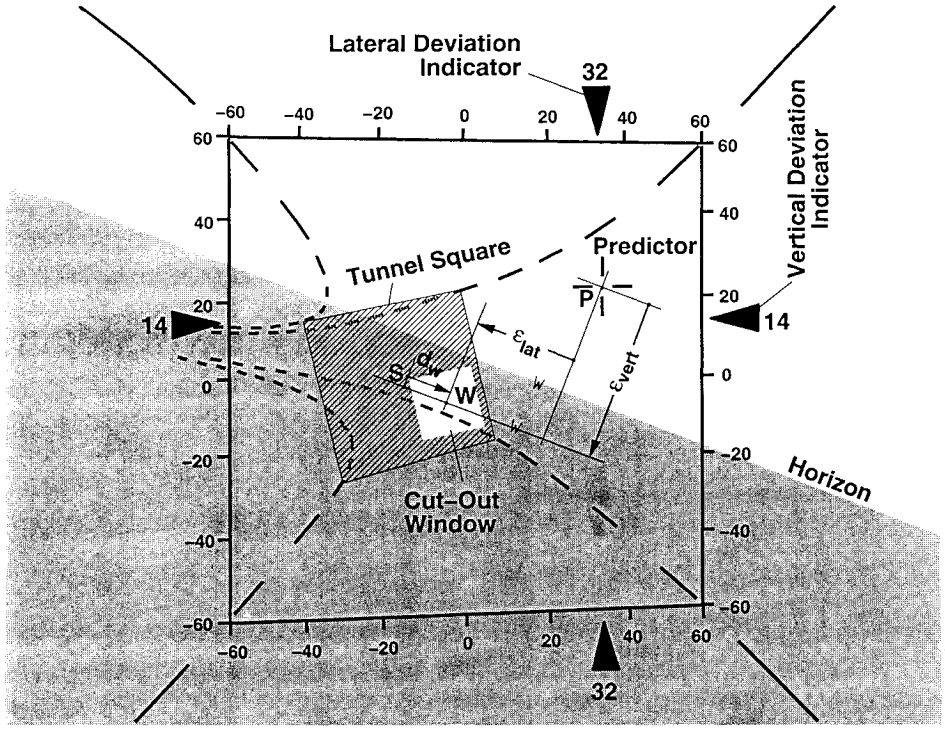

Fig. 1a Display layout of the improved tunnel display.

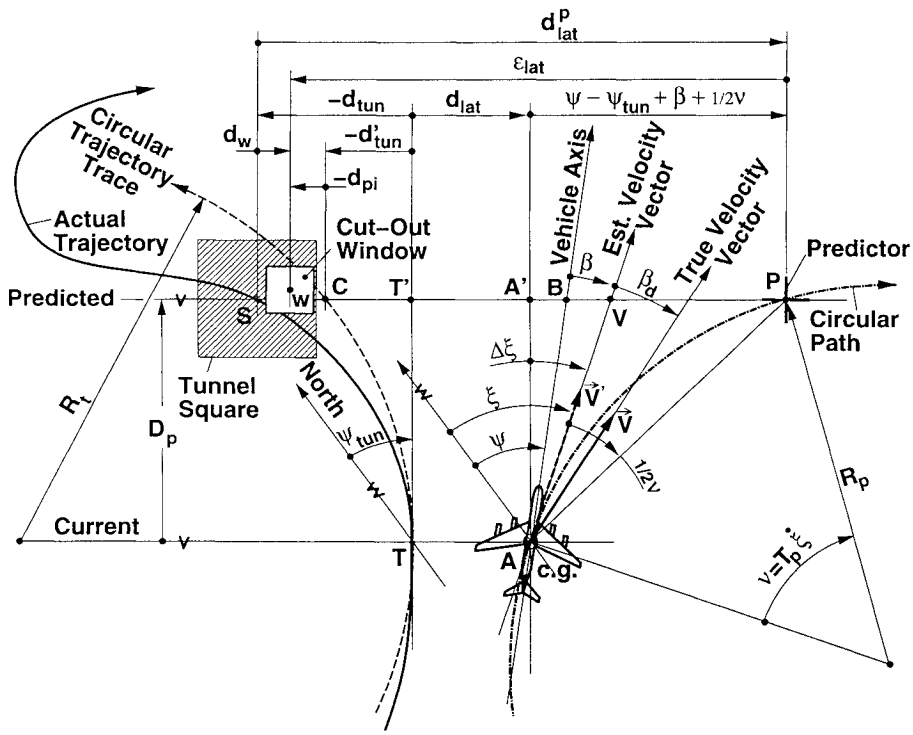

Fig. 1b Horizontal situation of the improved tunnel display.

position. A control strategy, aimed at keeping the cross centered at the square, would bring the future lateral and vertical deviations to zero. If the prediction was indeed correct, the actual deviations would eventually go to zero within several prediction time constants. Past experience[2,3] reveals that, for large and sluggish aircraft requiring long prediction times, this strategy results in poor positional accuracy in transitions from straight to curved trajectory sections and back and in the presence of low-frequency disturbances.

The improved guidance scheme is based on the use of an actively moving cutout reference window that is part of the tunnel square and one-quarter of its size, i.e., 75 ft in width, as shown in Fig. 1a. Rather than being placed at the center of the tunnel square S, the predictor is placed at the center of the cutout window W. The displacements of this cutout window with respect to the center of the tunnel square are minute and slow, but by providing the cutout window with the proper displacements, a highly improved predictor guidance law can be obtained. The signals that drive the cutout window are summarized hereafter.

The cutout window W is displaced in horizontal direction (parallel to the horizon) with respect to the center of the tunnel square S by the amount d_w, while the displacement in vertical direction is set to zero, as seen in Fig. 1b. The displacement d_w is composed of two

parts. The first part of d_w assists in improving curve transition behavior and corrects for corner cutting. This would require a guidance scheme that would keep the predictor symbol P on the circular dotted trajectory trace (point C), rather than on the actual trajectory (point S), as shown in Fig. 1b. This circular trace is tangential to the trajectory at the location T, with a radius R_t, which corresponds to the trajectory curvature at that location. This arrangement facilitates that, by appropriate lateral motion of the cutout window, i.e., the displacement between points S and C, in transitions from straight to curved sections, the onset of the banking cue will be delayed until the aircraft has actually reached the curved section. In sections with a constant curvature, however, the cutout window will remain centered at the tunnel square, and the situation will be identical to that of the original tunnel display.

The second part of d_w assists in reducing the effect of biases and/or low-frequency disturbances. It constitutes the output d_{pi} of a proportional-integral (PI) controller that has the actual measured lateral deviation as the input according to

$$d_{\text{pi}}(s) = -\frac{c(bs^2 + as + 1)}{s(s + d)} d_{\text{lat}}(s) \tag{1}$$

where the controller constants are chosen to be $a = T_p$, $b = 0.5T_p^2$, $c = 0.96$, and $d = 5.0$ for the given aircraft. Following Fig. 1b, the displacement d_w combining the two parts is given by

$$d_w = d_{\text{pi}} + d'_{\text{tun}} - d_{\text{tun}} \tag{2}$$

where d_{tun} is the portion of the predicted lateral deviation because of the actual trajectory shape and d'_{tun} is this portion referenced to the circular dotted trajectory trace. The displacement d_w constitutes the command input (or set point) to the control system. The lateral deviation of the predictor symbol P from the cutout window W constitutes the control error ε_{lat} that the pilot attempts to minimize.

A novel trajectory generation algorithm has been employed. The algorithm, which is discussed in detail in the theoretical companion paper,[10] creates a tunnel trajectory that best matches with the average vehicle response. The algorithm is based on experience with the original tunnel display that showed that a raw tunnel trajectory, composed of straight and curved sections with a constant radius, can be flown quite smoothly by bringing the predicted lateral and vertical deviations, d^p_{lat} and d^p_{vert}, to zero, provided the predictor distance D_p is chosen sufficiently large for the given vehicle dynamics. The predicted lateral deviation d^p_{lat} appears in Fig. 1a as the deviation of the predictor cross P from the center of the tunnel square S. The input to the algorithm is a raw trajectory, composed of straight sections, interconnected by circular arcs. This trajectory is flown by a paper aircraft and paper pilot in a disturbance-free fast-time simulation run. The paper pilot uses a well-tuned predictor and adequately chosen loop closure gain to follow the trajectory. The resulting three-dimensional vehicle path and bank angle response, form the basis for generating the spatial three-dimensional tunnel structure that exhibits smooth transitions from straight to curved sections and back and that is easily flyable by the actual aircraft.

Experimental Evaluation

Purpose of the Experiments

The purpose of the simulation studies was to evaluate the improved display layout and the improved predictor guidance scheme. It was of particular interest to evaluate the effectiveness of the cutout window display laws regarding the positional accuracy in transitions between straight to curved trajectory sections and in the presence of slow-varying side winds. Finally it was of interest to compare the human performance with the one of a well-designed autopilot. The autopilot in this study refers to the condition in which proportional control laws for the lateral and longitudinal control are employed, using the deviations of the predictor cross from the cutout window as control errors. The autopilot thus resembles a paper pilot in the sense that it models how the pilot would act on the deviations of the predictor cross from the cutout window. In all of the simulations, the mentioned novel trajectory generation algorithm has been used to create smooth and flyable trajectories that best match with the average vehicle response.

Experimental Setup

The simulations were carried out in a fixed-base simulator setup, using an Silicon Graphics IRIS 4D/70 GT graphics workstation. The image shown in Fig. 1a, without the explanatory parameter labels but with the horizontal and vertical displacement indicator labels, was presented on a display monitor measuring 19 in. diagonally. The update rate was about 20–25 Hz. The shaded tunnel square shown in Fig. 1a was drawn as a semitransparent surface. The trajectory generation algorithm discussed in the theoretical companion paper[10] was used to generate the horizontal, vertical, and roll profile of the tunnel. Thus, the tunnel was banked in curves, and the bank angle matched the bank angle of the aircraft needed for making a coordinated turn at the given airspeed. A Measurement Systems, Inc., two-axis spring-loaded high precision side stick was used as the input device. A lateral stick deflection represented a roll-rate command, whereas a forward-aft deflection represented a pitch-attitude command. A simplified linearized trim model of a large transport aircraft (DC-8) was used. The lateral vehicle dynamics included the spiral divergence, roll-subsidence, and Dutch-roll modes, and the longitudinal dynamics the short-period and phugoid modes. The dimensional stability derivatives were obtained from Ref. 11. The lateral dynamics were augmented by a roll-rate command system, Dutch-roll damper and turn coordinator, and the longitudinal dynamics by a pitch-attitude command system with autothrottle loop to keep the airspeed at a constant value of 220 ft/s. Furthermore, the longitudinal dynamics included a PI controller with a time constant of 10 s, for autotrim adjustment during vertical trajectory profile changes.

Experimental Design

The experimental parameters are the display configuration, the prediction time T_p, and the flight condition. Two display configurations were compared: the original configuration, in which the cutout window was fixed in the center of the tunnel cross-section square, and the improved configuration, in which the cutout window was driven by the guidance laws discussed earlier. The nearby tunnel cross-section square was at all times located at 2-s prediction time ahead. For the distant square, accommodating the predictor cross, three prediction times were investigated: 3, 6, and 9 s ahead. Two flight conditions were considered: a condition in which no disturbances were present and one in which both turbulence and steady crosswinds were present. The no-disturbances condition allowed the evaluation of the tunnel following characteristics in transitions from straight to curved trajectory sections and back, whereas the condition with disturbances allowed the evaluation of the behavior in the presence of turbulence and slowly varying side winds.

The turbulence p_{gust} was introduced on the roll rate and was created by passing Gaussian zero mean white noise through a cascade of a first- and a second-order filter. The break frequency of the first-order filter was 4 rad/s and the natural frequency of the second-order filter was 0.8 rad/s with a damping factor of $\zeta = 0.5$. The root-mean-square (rms) value of p_{gust} was about 1.75 rad/s. The second-order filter, which added disturbances in the lower frequency range, i.e., <0.8 rad/s, allowed increasing the power of the disturbance, without having too much power in the high frequencies. It also compensated for the fact that the disturbances on other states, i.e., a side wind gust v_{gust} and a yaw gust r_{gust}, were not taken into account.

The crosswinds were steady and randomly selected to come from either one of the four main wind directions, with a magnitude of 20 ft/s. The sideslip angle was assumed to be measured onboard with respect to the air mass rather than to a ground-based reference. This will result in an error in the predicted vehicle position that is proportional to the magnitude of the crosswinds. Since the vehicle heading angle changes along the trajectory, the magnitude of the crosswinds will change accordingly, which is experienced as a slowly varying disturbance. Each trajectory was started with a zero position offset and an initial heading that was parallel to the tunnel.

Because the repeated flying of one particular trajectory profile would result in familiarization of the subjects with the trajectory and would therefore affect the general validity of the results, eight different trajectory shapes were used. A plan view of four of these approach trajectories, before applying the smoothing algorithm, is shown in Fig. 2a, and the descent profiles are shown in Fig. 2b.

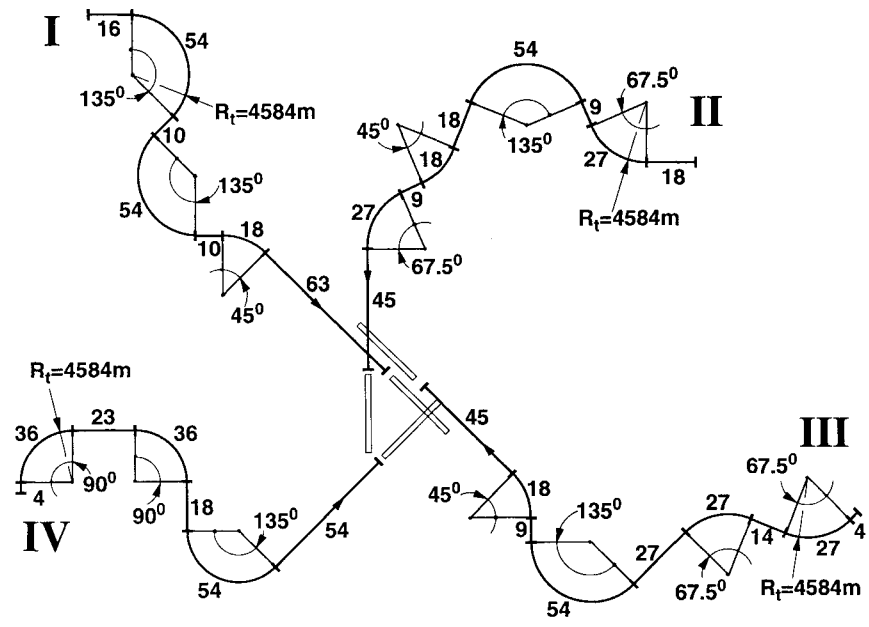

Fig. 2a Plan view of the approach trajectories: length of section is indicated in units of 200-ft length.

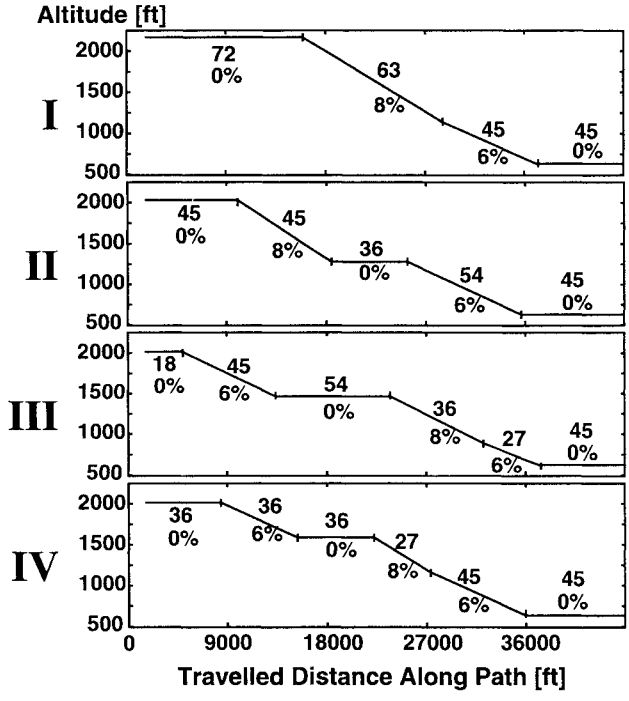

Fig. 2b Descent profiles of the approach trajectories: length of section is indicated in units of 200-ft length.

The other four trajectories were exact mirror images and are not drawn. Each trajectory is composed of a total of nine straight and curved sections. The numbers near each section represent its length in units of 200 ft length. Total trajectory length was 55,000 ft, and each approach lasted 250 s. The sequence in which the trajectories were flown was randomized. Note that the trajectories were deliberately chosen to be far more active than commonly used microwave landing system approaches. This was done to evaluate the improved predictor guidance scheme under worst-case circumstances.

The experimental design was a full factorial of 12 experimental conditions: two display configurations (original, improved), times three predictor distances (3, 6, and 9 s), times two flight conditions (no disturbances, with disturbances). Eight subjects participated in the experiment. Each one of the 12 conditions was repeated four times by each one of the subjects.

Table 1 Subject background

Subject	Sex	Age	Flight hours	Aircraft
WG	M	41	1000	T-28, S-2
DL	M	29	3200	C-172, PA-30, DHC-6-300
BL	F	27	2000	DHC-6-300, B-20, B-30, C-172, C-152, P-144
GR	M	33	2600	C-182, C-172, C-152, BE-76, Piper Warrioir
KB	M	24	460	Piper Dakota, Piper Archer
MW	M	30	800	Asel, Amel
SG	M	37	9000	DC-10
BR	M	47	1500	C-172, Piper

Subject Background, Training, and Experimental Procedure

The subjects consisted of seven male and one female general aviation pilots ranging in age between 24 and 47 years. The subject background is summarized in Table 1. Subject training for each subject lasted 2–3 h, in which each one of the experimental configurations was addressed at least once. Production runs were carried out in groups of four repetitions for each configuration. Although the turbulence sequence, which originated from a pseudorandom noise generator, was chosen to be different for each run, the root-mean-square value was kept constant. The configurations were addressed in a random sequence that was different for each subject. The tunnel trajectories were also addressed in a random sequence, but in a manner that each configuration was flown for each trajectory four times (by four different subjects).

The subjects were instructed to minimize the actual lateral and vertical deviations from the tunnel center. They were briefed about the function of the predictor and the cutout window guidance information. They were informed that a possible guidance law was to keep the predictor cross centered at the cutout window, but they were left free to choose their own strategy for minimizing the actual deviations from the trajectory.

Experimental Measurements

For every run the time histories of the following signals were recorded: the actual lateral and vertical deviations of the aircraft from the center of the tunnel, d_{lat} and d_{vert}, respectively; the lateral and vertical deviation of the predictor cross from the cutout window, ε_{lat} and ε_{vert}, respectively; the vehicle roll angle ϕ and the roll-rate p; and the lateral and forward-aft stick deflections.

Integral run scores for the combined actual lateral and vertical deviation and the combined lateral and vertical deviation of the

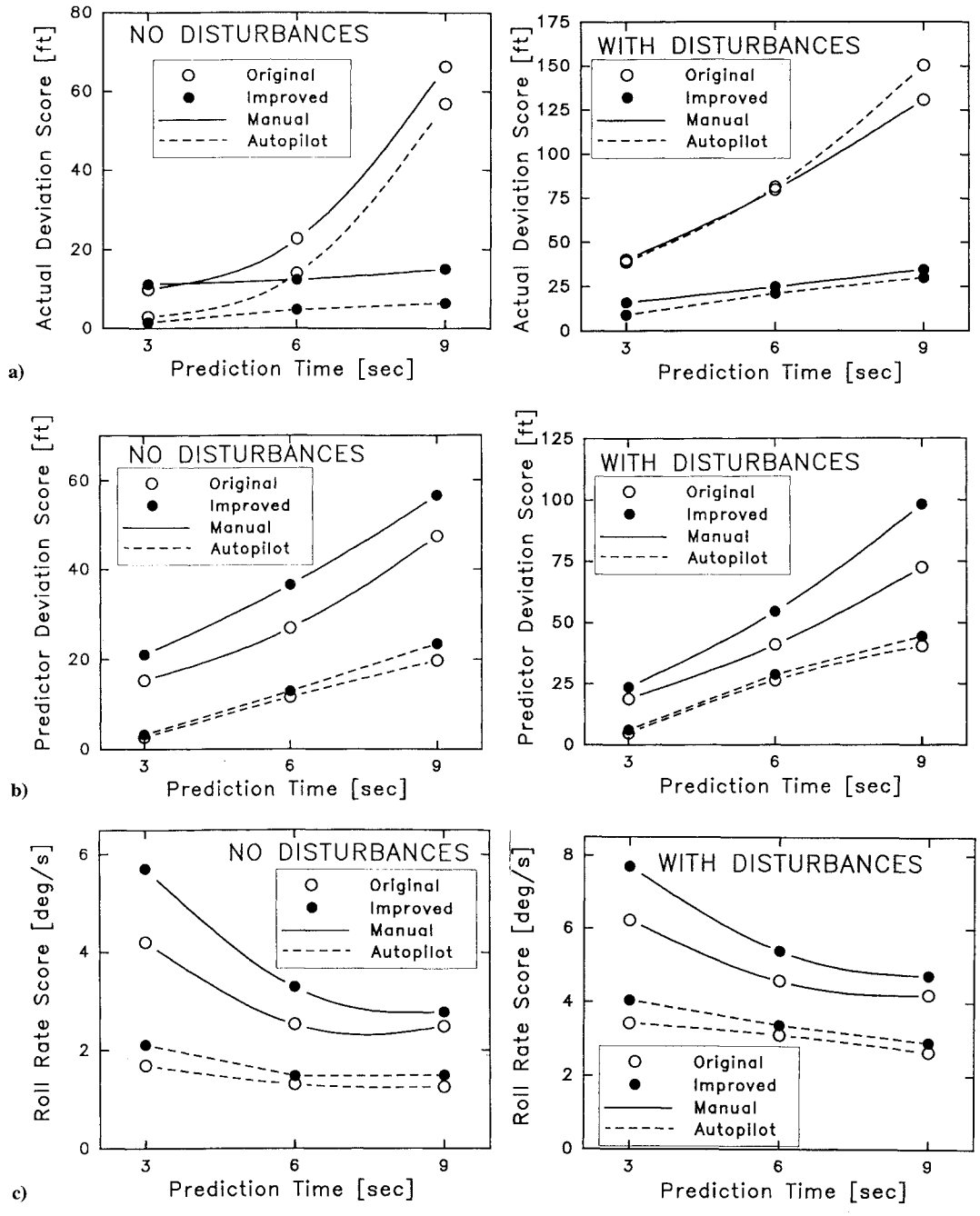

Fig. 3 Averaged integral run scores as a function of the prediction time T_p: a) actual deviation scores, b) scores for deviation of predictor cross from cutout window, and c) roll-rate activity scores.

predictor cross from the cutout window, are computed according to

$$s_d = \sqrt{\frac{1}{T}\int_{t=0}^{T}\left(d_{\text{lat}}^2 + d_{\text{vert}}^2\right)\mathrm{d}t}$$
$$s_\varepsilon = \sqrt{\frac{1}{T}\int_{t=0}^{T}\left(\varepsilon_{\text{lat}}^2 + \varepsilon_{\text{vert}}^2\right)\mathrm{d}t} \tag{3}$$

and an integral run score for the roll-rate activity is computed according to

$$s_p = \sqrt{\frac{1}{T}\int_{t=0}^{T} p^2\,\mathrm{d}t} \tag{4}$$

where T is the duration of the run.

Since the vehicle was essentially rate controlled in roll, the roll-rate score was found to be almost proportional to the score of the lateral stick command. Since the vehicle roll-rate reflects general vehicle motions, rather than the displacements of a manipulator with a specifically chosen stick gearing, the roll-rate activity was chosen as the representative score for pilot activity.

Experimental Results

The averaged run scores for the actual deviation, the deviation of the predictor cross from the cutout window, and the roll-rate activity are plotted in Figs. 3a–3c as a function of the prediction time T_p. The results for the no-disturbances condition, shown in the left-hand part of the figures, reflect the tunnel following performance in transient sections, whereas the results for the with-disturbances condition, shown in the right-hand part of the figures, reflect the performance in the presence of turbulence and low-frequency disturbances. Each data point in the figure represents the average of a set of 32 runs, i.e., four repetitions, performed by each one of the eight subjects,

where each one of the eight approach trajectories was flown four times (by four different subjects).

In Figs. 3a–3c the results for automated flight are indicated by the dotted lines. Proportional control laws for the lateral and longitudinal control are employed, using the deviations of the predictor cross from the cutout window as control errors. The gain for the lateral control $K_\varepsilon^{\text{lat}}$ is optimized for each one of the three prediction times to obtain a fast and well-damped system response. Thus $K_\varepsilon^{\text{lat}}$ was chosen to be 0.02, 0.003125, and 0.00175 for the 3-, 6-, and 9-s predictor, respectively. The remaining parameters were chosen to be identical to the manual control situation. The results for automated flight in Figs. 3a–3c represent the average of a set of eight runs, in which each one of the trajectories was flown once.

Comparison Between Autopilot and Manual Response

Figures 3a–3c show a strong similarity between the autopilot and the manual subject response in the shape of the scores vs prediction time curves. This indicates that, like the autopilot, the subjects might have employed a proportional control law on the deviation of the predictor cross from the cutout window. The curves for the manual control are generally shifted upward. The largest difference between autopilot and manual response is found in the roll-rate activity score s_p for $T_p = 3$ s. A possible explanation for this difference is that the subjects are not able to generate the relatively large system gain $K_\varepsilon^{\text{lat}}$ necessary for stabilizing the system. A root locus analysis in the theoretical companion paper[10] showed that an insufficient gain will result in badly damped system poles close to the origin. This finding was also confirmed by the subjects, who commented that a tendency existed for developing low-frequency pilot induced oscillations for this configuration. The general upshift of the curves may also be attributed to human operator remnant noise inherently present in human control actions.[12]

Effect of the Predictor Distance

Figure 3b shows that for all configurations the predictor deviation score s_ε increases almost linearly with the prediction time T_p. This indicates that for the given perspective display the subjects acted on the visual angle subtended between the predictor cross and the cutout window, rather than on the predicted deviation per se.

For the original predictor, the actual deviation score s_d is found to increase progressively with T_p, which demonstrates the earlier mentioned degraded performance for increased prediction times, see Fig. 3a. On the other hand, the roll-rate activity shown in Fig. 3c generally decreases with T_p. This finding is easily verified by realizing that as T_p increases, the predictor lead zeros are located closer to the origin, resulting in a lower system gain and a better damped system. This confirms the findings of earlier work[2,3] that with the original predictor the positional accuracy and control activity reduce with an increase in T_p. Therefore, the tuning of the prediction time involves compromising between sufficient tunnel following accuracy on one hand and reasonable control activity on the other hand. Past experience has shown that this tuning process did not always achieve satisfactory results.

Comparison of Original with Improved Predictor

Figure 3a shows that for the improved predictor and for the no-disturbances condition, the curves for the actual deviation score are almost flat. At $T_p = 9$ s the improved predictor yields a markedly lower actual deviation score than the original predictor. The left-hand part of Fig. 3a also shows that the trends in deviation score for autopilot and manual control are identical and that the manual curves are shifted upward by about 10 ft. The left-hand part of Fig. 3c shows that the improved predictor yields an increased roll-rate activity that becomes progressively larger with a decrease in the prediction time T_p. For $T_p = 3$ s (no-disturbances condition), the improved predictor yields a markedly increased roll-rate activity with no improvement in tunnel following accuracy. This means that for small prediction times the improved predictor has no advantage. Since for the larger prediction times the improved predictor yields a highly improved trajectory following accuracy, with no increase in roll activity, the improved predictor is the most effective for the larger prediction times. For the no-disturbances condition, the improved trajectory following accuracy is equivalent with improved transient behavior.

The curves for the predictor deviation score s_ε in Fig. 3b show that the autopilot is more consistent in keeping the predictor cross centered at the cutout window than the subjects. For the autopilot, there is no difference in scores between the original and improved predictor. For manual control the deviations are larger for the improved predictor, indicating that the pilot either deliberately chose not to follow a proportional control strategy or that larger errors developed because of increased human operator noise as a result of the increased activity in the control task.

Figure 3a shows that for the with-disturbances condition, the improved predictor yields markedly reduced actual deviation scores for all three prediction times. Like for the no-disturbances case, the contribution of the improved predictor is the largest for $T_p = 9$ s. The ability of the improved predictor to reduce the effect of low-frequency disturbances mainly depends on the PI controller action. The controller parameters are chosen so that the integral action is fast enough to cope with the slow-varying disturbance during the turn on one hand and to yield an acceptable pilot response on the other hand.

Figure 3a also shows that the actual deviation scores for autopilot and manual control are almost identical. Observe that for the original predictor and for $T_p = 9$ s the subjects performed better than the autopilot. This indicates that, in contrast to the autopilot and in view of the deficiencies of the original predictor at large prediction times, the subjects did not use a proportional control law on the predicted lateral deviation. This confirms the findings of earlier work[3] that in the presence of a deficient predictor the pilots rely more on the tunnel image.

The curves for the with-disturbances condition shown in Fig. 3b for the predictor deviation scores show a close resemblance with the no-disturbances condition. Also for the with-disturbances condition, the autopilot is more consistent in keeping the cross centered at the cutout window square. The curves shown in Fig. 3c for the roll-rate activity show that also for the with-disturbances condition the improved predictor yields a larger roll-rate activity.

Discussion of Results

The experimental results reflect the operator performance in a relatively narrow, part-task, fixed-base simulation. A simplified linear vehicle model was used, abstracted from the dynamics of a DC-8 aircraft. Aircraft controls were limited to a simple, two-axis control manipulator. Roll and pitch scales, as well as explicit altitude and vertical speed information, were not shown on the display. The introduction of large low-frequency disturbances into the system was modeled by basing the computation of the predicted vehicle position on air mass referenced sideslip measurements rather than on ground-based ones, a situation that might be too pessimistic in view of the onboard availability of inertial measurement unit data.

However, a large part of the full-scale task will deal with the manual tracking of the tunnel. In spite of the mentioned experimental limitations, the results generally show that the improved predictor guidance law combines the advantage of the 9-s predictor, yielding a well-damped system with a low system gain, with very good transition curve flying characteristics and insensitivity to low-frequency disturbances. The cost of a slightly increased roll-rate activity for the improved predictor is small in view of the highly improved positional accuracy. Pilots commented that, although the improved predictor required slightly more control activity, it was still very easy to fly.

Motion cues are expected to add damping to the system and therefore constrain the roll-rate activity. For the smaller prediction times this might limit the loop closure gain, that, for the improved guidance scheme, might result in low-frequency instability. For the 9-s predictor for which the improved scheme is the most effective, however, the roll-rate activity is hardly affected by the cutout window guidance law. For this situation, motion cues are not expected to significantly impact the findings of this study.

Note that the use of an air mass referenced sideslip measurement does not suggest the direct use of the raw air mass referenced sideslip measurement in the display. The purpose of this choice was

to create a worst-case condition in which the improved predictor scheme could be tested. For large aircraft, the ground-based referenced sideslip measurement is usually available from an inertial measurement unit. Nevertheless, the predicted vehicle position remains still susceptible to measurement errors, in particular for the larger prediction times. Implementation of the display in the actual aircraft requires a review of the available measurements and the development of filtering or estimation schemes that would impart the required signals to the display. For example, the measurement of the acceleration cues, necessary for defining the predicted vehicle path curvature, can be based on intertial measurements[4,5] or on measurements relative to the air mass.[9] The air mass referenced measurements have the distinct advantage of providing relevant safety margin information to the pilot in the presence of wind shears.[9]

Although roll and pitch scales, as well as explicit vertical position and rate information, are an essential part of acceptable flight displays, their effect on the dynamic evaluation of the predictor schemes is believed to be small. The integration of this information in the existing format is a display design issue. Past experience has shown that this information can be integrated effectively in the off-center areas of the display, without affecting the predictor guidance information in the central area.

Conclusions

The cutout window guidance information yields a superior performance for the larger prediction times in transitions to and from curved trajectory sections. The integral control action imparted to the cutout window greatly reduces cross track errors resulting from low-frequency disturbances, biases, or errors inherently present in the system because of a slightly higher control activity.

The advantages of the circular path predictor, as implemented in the original tunnel display versions, of flying prolonged curves with zero steady-state errors are still present in the improved version. The pilot is able to ignore the guidance cutout window and use the center of the square as a reference. In entry maneuvers and in maneuvers in which the square is out of view, the predictor acts as in the original versions: the predictor is globally placed on the desired future position and the predictor lead zeros act to stabilize the system.

The guidance information imparted to the cutout window modifies the effectively controlled element. Thus, an improperly chosen cutout window guidance law, e.g., excessive integral control action, could possibly adversely affect the tracking workload. An increased workload, in turn, might impair the spatial awareness, since the pilot might need to allocate more attention to the cutout window than to the overall aircraft spatial situation. Therefore, the dynamics of the cutout window should be designed so that the cutout motions and the motions of the predictor are separated in frequency. This, in turn, will set a constraint on the amount of integral control action that can be imparted to the cutout window motions.

Acknowledgments

This research has been partially supported by a grant from the Aerospace Human Factors Research Division, NASA Ames Research Center, Moffett Field, California, under cooperative agreement No. NCCW-9. Stephen R. Ellis of NASA Ames Research Center has been the Scientific Monitor for this grant. The flight simulation experiments were performed during the author's National Research Council Associateship at NASA Ames Research Center. The author wishes to thank the pilot subjects for their time, efforts, and valuable comments.

References

[1]Grunwald, A. J., "Predictor Laws for Pictorial Flight Displays," *Journal of Guidance, Control, and Dynamics*, Vol. 8, No. 6, 1985, pp. 545–552.

[2]Grunwald, A. J., Robertson, J. B., and Hatfield, J. J., "Experimental Evaluation of a Perspective Tunnel Display for Three-Dimensional Helicopter Approaches," *Journal of Guidance and Control*, Vol. 4, No. 6, 1981, pp. 623–631.

[3]Grunwald, A. J., "Tunnel Display for Four-Dimensional Fixed-Wing Aircraft Approaches," *Journal of Guidance, Control, and Dynamics*, Vol. 7, No. 3, 1984, pp. 369–377.

[4]Baxter, J. R., and Workman, J. D., "Review of Projected Displays of Flight Information and Recommendations for Further Developments," Australian Defense Scientific Service Aeronautical Research Lab., ARL/HE2, Melbourne, Australia, 1962.

[5]Gold, T., "Quickened Manual Flight Control with External Visual Guidance," *IEEE Transactions on Aerospace and Navigational Electronics*, Vol. ANI-11, Sept. 1964, pp. 151–156.

[6]Bray, R. S., "A Head-Up Display Format for Application to Transport Aircraft Approach and Landing," NASA TM-81199, 1980.

[7]Bray, R. S., and Scott, B. C., "A Head-Up Display Format for Transport Aircraft Approach and Landing," NASA CP-2170, 1980.

[8]Merrick, V. K., "Simulation Evaluation of Two VTOL Control/Display Systems in IMC Approach and Shipboard Landing," NASA TM-85996, 1984.

[9]Hynes, C. S., Franklin, J. A., Gordon, H. H., Martin, J. L., and Innis, R. C., "Flight Evaluation of Pursuit Displays for Precision Approach of Powered-Lift Aircraft," *Journal of Guidance, Control, and Dynamics*, Vol. 12, No. 4, 1989, pp. 521–529.

[10]Grunwald, A. J., "Improved Tunnel Display for Curved Trajectory Following: Control Considerations," *Journal of Guidance, Control, and Dynamics*, Vol. 19, No. 2, 1996, pp. 370–377.

[11]McRuer, D., Ashkenas, I., and Graham, D., *Aircraft Dynamics and Automatic Control*, Princeton Univ. Press, Princeton, NJ, 1973, pp. 711–717.

[12]Kleinman, D. L., Baron, S., and Levison, W. H., "An Optimal Control Model of Human Response, Part I: Theory and Validation. Part II: Prediction of Human Performance in a Complex Task," *Automatica*, Vol. 6, 1970, pp. 357–369.